Cell Reports
Physical Science

CellPress
OPEN ACCESS

Perspective

Formation and stabilization of metastable halide perovskite phases for photovoltaics

Shuangyan Hu,[1,3] Arnauld Robert Tapa,[2,3,*] Xuechang Zhou,[4] Shuping Pang,[5] Monica Lira-Cantu,[6,*] and Haibing Xie[3,*]

SUMMARY

Halide perovskites are semiconductors that have impacted the photovoltaic field in single and multijunction devices. Among them, metastable $FAPbI_3$-based (FA, formamidinium) and $CsPbI_3$-based perovskites are frontrunner materials for perovskite solar cells. However, they face the same challenge; their photoactive black perovskite phases spontaneously transform into the yellow non-photoactive δ phases at room temperature. Synthesizing and stabilizing the pure perovskite phase has been a great challenge, leading to frequent updates of the reported record efficiency and stability for organic-inorganic hybrid perovskite and all-inorganic perovskite photovoltaics. In this perspective, we first discuss the material properties of metastable perovskites $FAPbI_3$ and $CsPbI_3$ and later review the most relevant strategies currently employed for obtaining and stabilizing these perovskite phases. Finally, we summarize the thermodynamic changes taking place during transition processes and outlook on the potential applications and scalability of these metastable perovskites.

INTRODUCTION

Metal halide perovskites have attracted extensive research interest in solar cells, light-emitting diodes, and detectors, owing to their outstanding optoelectronic properties such as long carrier diffusion length, tunable band gaps, and high defect tolerance.[1–6] In 2009, perovskite solar cells (PSCs) with power conversion efficiency (PCE) of 3.8% were first reported based on $MAPbI_3$ (MA, methylammonium) and $MAPbBr_3$ perovskite materials.[1] In recent years, $FAPbI_3$-based perovskites (FA, formamidinium; with small amounts of dopants such as MA^+, Cs^+, or Br^-) have presented the best efficiency values of PSCs. They also possess enhanced stability due to their ideal band gaps and an outstanding thermal stability if compared to the $MAPbI_3$ perovskite (Figure 1A).[2,7–11] The highest certified PCE of PSCs belongs to $FAPbI_3$-based perovskites with 26.1% record efficiency.[12]

Inorganic perovskites with good thermal stability are attracting enormous interest in photovoltaics.[2] In particular, $CsPbI_3$-based perovskites (pure $CsPbI_3$ or with a small amount of dopants such as Br^-) with low band gap among Pb-based inorganic perovskites are guiding the best PCE of inorganic PSCs to 21% (Figure 1B).[13] $CsPbI_3$-based perovskites also show huge potential for their application in tandem solar cells due to their ideal band gap and outstanding ability of anti-phase segregation.[14]

However, $FAPbI_3$ and $CsPbI_3$ are currently facing the same challenge observed for their black photoactive perovskite phases, namely the spontaneous transformation into the yellow non-photoactive δ phase at room temperature (RT).[2,15,16] The

[1]Institute of Microscale Optoelectronics, Shenzhen University, Shenzhen 518060, China

[2]College of Civil and Transportation Engineering, Shenzhen University, Shenzhen 518054, China

[3]Institute for Advanced Study, Shenzhen University, Shenzhen 518060, China

[4]College of Chemistry and Environmental Engineering, Shenzhen University, Shenzhen 518071, China

[5]Qingdao Institute of Bioenergy and Bioprocess Technology, Chinese Academy of Sciences, Qingdao 266101, China

[6]Catalan Institute of Nanoscience and Nanotechnology (ICN2), CSIC and the Barcelona Institute of Science and Technology (BIST), Building ICN2, Campus UAB, 08193 Bellaterra, Barcelona, Spain

*Correspondence:
tapaarnauld@szu.edu.cn (A.R.T.),
monica.lira@icn2.cat (M.L.-C.),
xhbxal2021@szu.edu.cn (H.X.)

https://doi.org/10.1016/j.xcrp.2024.101825

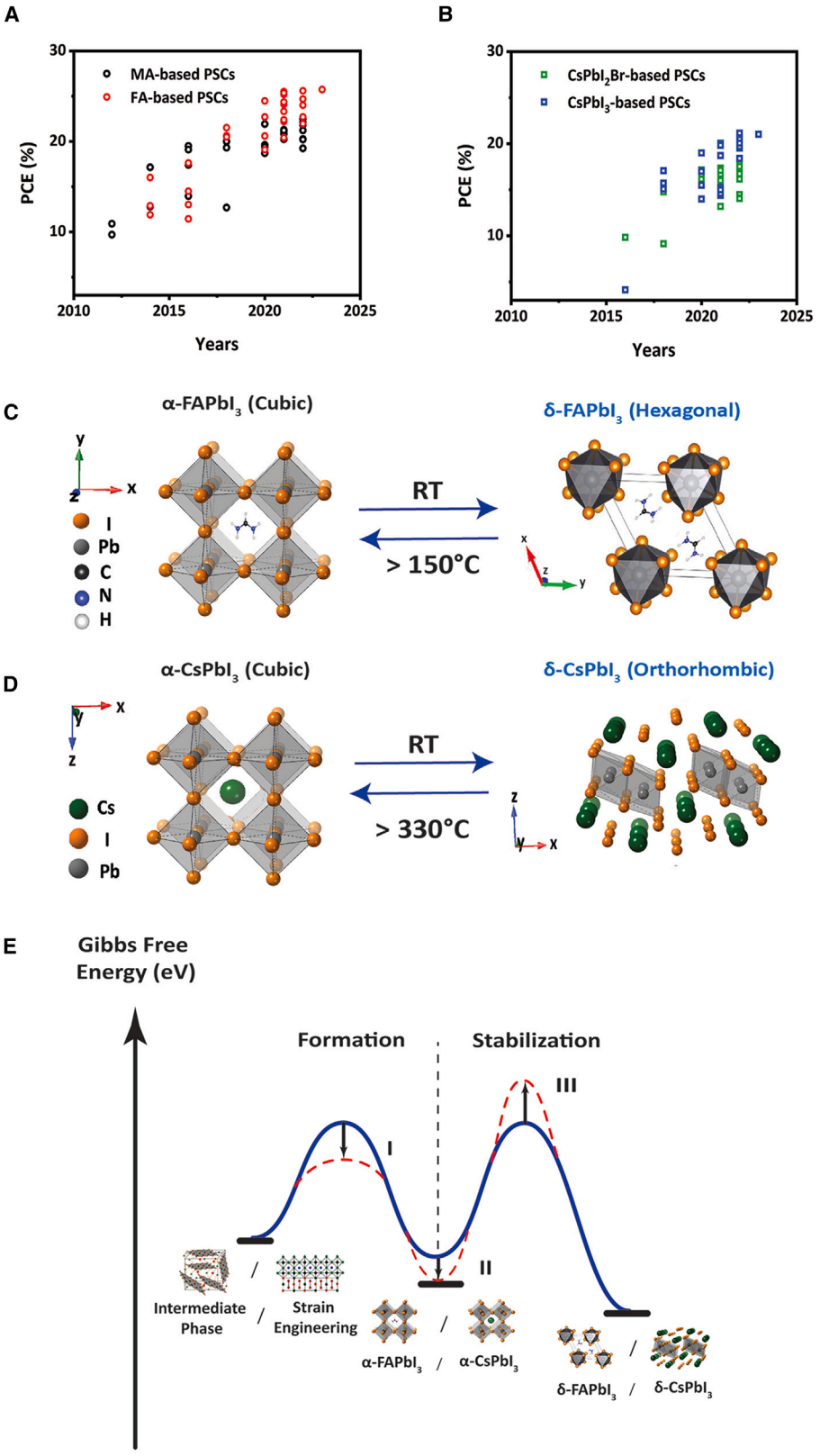
A
MA-based PSCs
FA-based PSCs
PCE (%)
Years
B
CsPbI2Br-based PSCs
CsPbI3-based PSCs
PCE (%)
Years
C
α-FAPbI3 (Cubic)
δ-FAPbI3 (Hexagonal)
RT
> 150°C
I
Pb
C
N
H
D
α-CsPbI3 (Cubic)
δ-CsPbI3 (Orthorhombic)
RT
> 330°C
Cs
I
Pb
E
Gibbs Free Energy (eV)
Formation
Stabilization
I
II
III
Intermediate Phase
Strain Engineering
α-FAPbI3
α-CsPbI3
δ-FAPbI3
δ-CsPbI3

Figure 1. Brief introduction to $FAPbI_3$ and $CsPbI_3$

(A and B) PCE evolution reported from 2010 to 2023 for hybrid organic-inorganic (FA- and MA-based) and inorganic ($CsPbI_3$- and $CsPbI_2Br$-based) PSCs.
(C and D) Phase transition of $FAPbI_3$ and $CsPbI_3$ (α phase to δ phase) at high temperatures and room temperature, respectively.
(E) Thermodynamic changes of phase transition for the formation and stabilization processes of $FAPbI_3$ and $CsPbI_3$ metastable perovskite phases. Process I: reducing the formation energy barrier of the metastable perovskites by intermediate-phase engineering, strain engineering, and two-step method. Process II: decreasing the Gibbs free energy is beneficial for the formation and stabilization of the metastable perovskites. Process III: increasing energy barrier to suppress the phase transition from perovskite phases to non-perovskite phases. The δ and α symbols in this figure indicate the hexagonal non-perovskite and 3D perovskite polymorphs, respectively. This notation does not imply anything about the underlying crystallographic symmetry of the perovskite phase.

formation and stabilization of metastable $FAPbI_3$ and $CsPbI_3$ black perovskites results in the increase of PCEs and an enhanced device stability for both the organic-inorganic hybrid perovskites and the inorganic perovskites.[9,17,18]

In this perspective, we first summarize the different types of perovskite phases and their unique phase transitions as well as the corresponding mechanisms observed on the formation of $FAPbI_3$ and $CsPbI_3$. In addition, we review the different formation strategies to obtain the metastable pure-phase perovskite films (including intermediate-phase engineering, strain engineering, and two-step method) and present the most recent developments reported in the literature, considering a compositional, dimensional, additive, and surface engineering point of view. Next, we analyze the future challenges that we are currently required to overcome to increase our understanding of phase formation and stabilization. Finally, we summarize the thermodynamic energy changes during the transition process of metastable perovskite phases and discuss the potential applications of metastable perovskites.

MATERIAL PROPERTIES

Properties of $FAPbI_3$

$FAPbI_3$ is characterized by its two main phases: a metastable black cubic perovskite phase (α phase, space group *Pm*3*m*) obtained at high temperature (over 150°C) and a stable yellow hexagonal non-perovskite phase (δ phase, space group $P6_3mc$) observed at RT (Figure 1C).[2] α-$FAPbI_3$ is considered one of the best candidates for PSCs as it exhibits an ideal band gap (1.48 eV), very close to the optimal band gap of 1.4 eV in the Shockley-Queisser limit curve, which can theoretically achieve a device efficiency of above 32%.[19–21] Furthermore, α-$FAPbI_3$ in comparison with the traditional $MAPbI_3$ perovskite has excellent thermal stability that meets the requirements for its application in PSCs.[2,20] The acquisition of α-$FAPbI_3$ films generally requires a high phase-transition temperature, which can also lead to the partial decomposition of $FAPbI_3$ into PbI_2.[20] The entropy contribution of the organic cation to the Gibbs free energy plays a crucial role in the selection of structure and stability of $FAPbI_3$ perovskite.[15] In high-temperature α-$FAPbI_3$, the FA^+ cations have isotropic orientation with large entropy, which stabilizes the cubic structure. Upon cooling, the FA^+ cations acquire strong preferential orientation in the hexagonal phase with lower entropy.[15]

Properties of $CsPbI_3$

$CsPbI_3$ perovskite with a band gap of ~1.73 eV is the most typical and popular material among highly efficient inorganic PSCs. $CsPbI_3$ has three photoactive black perovskite phases, the cubic (α) phase (space group: *Pm*3*m*), tetragonal (β) phase (space group: *P*4/*mbm*), and orthorhombic (γ) phase (space group: *Pbnm*), and a more thermodynamically stable "yellow" orthorhombic (δ) phase at RT (Figure 1D).[2,16] The α phase of $CsPbI_3$ can be obtained under 360°C. With the decrease of temperature to 260°C and 175°C, the α phase transforms into the

lower-symmetry β phase and γ phase, respectively, with the increasing tilt of PbX_6 octahedral.[22] At RT, these desirable black phases spontaneously transform into a yellow non-perovskite phase with a band gap (E_g) of 2.82 eV. It is widely reported that the phase instability of black $CsPbI_3$ mainly originates from the large lattice distortion of the octahedral perovskite structure with a low tolerance factor of 0.81.[23,24]

Progress and challenges of metastable perovskite phases

Even though a popular explanation of the instability of perovskite phases for $FAPbI_3$ and $CsPbI_3$ is their high (0.987) or low (0.81) tolerance factor, the mechanism behind the phase stabilization of the $FAPbI_3$ and $CsPbI_3$ perovskites at high temperatures is still under debate in the scientific community. The stable perovskite phase of $FAPbI_3$ under high temperature has been attributed to the isotropic orientation of FA^+ cation with large entropy.[15] Nevertheless, there is no clear understanding of the isotropic orientation mechanism for the cubic-to-hexagonal structural phase transition of the $CsPbI_3$ perovskite under different temperatures. The phase transition is determined by the thermodynamic stability of the yellow non-perovskites and black perovskites. Until now, most reports have focused on the discussion about the black perovskite phases, and thermodynamic studies about the yellow non-perovskite phases get less attention and thus need more comprehensive research.

FORMATION OF $FAPbI_3$- AND $CsPbI_3$-BASED PEROVSKITE PHASES

The high energy barrier of the transformation from yellow phase to black phase restrains the formation of pure black $FAPbI_3$-based and $CsPbI_3$-based perovskite phases.[25,26] Intermediate-phase engineering, strain engineering, and the two-step solution method play important roles in promoting the formation of their black perovskite phases by reducing the formation energy barrier (process I in Figure 1E).[20,27]

Intermediate-phase engineering

Formation of intermediate phases by introducing volatile additives in $FAPbI_3$-based and $CsPbI_3$-based precursor films can avoid the generation of the yellow δ phases and reduce the formation energy barrier of the perovskite phases, promoting the formation of the pure black perovskite.[27]

In early PSC research, MACl and FACl were used to prepare the α-$FAPbI_3$ phase. In the process, the 1:1 ratio of $FAPbI_3$/additive was commonly used in the precursor solution, allowing the formation of an intermediate phase of $FAPbI_3$-MACl or $FAPbI_3$-FACl. These intermediate phases prevent the formation of the yellow phase and promote the direct transformation into the black $FAPbI_3$ perovskite phase once the MACl or FACl is removed during the annealing process (Figure 2A).[26]

Consequently, the role of MACl additive on the perovskite crystal structure was investigated based on three major aspects as follows.[30]

(1) Cl thermodynamically stabilizes the $FAPbI_3$ perovskite structure by enhancing the intensity of the *p* orbital of I at the HOMO state, leading to a strengthened interaction between FA and I.
(2) MA^+ allows total volume shrinkage of the incorporated $FAPbI_3$ perovskite system compared to the system without MA^+. Moreover, it contributes to the lower formation energy of the incorporated system, thanks to the dipole moment of MA^+, which is ten times larger than that of FA^+.

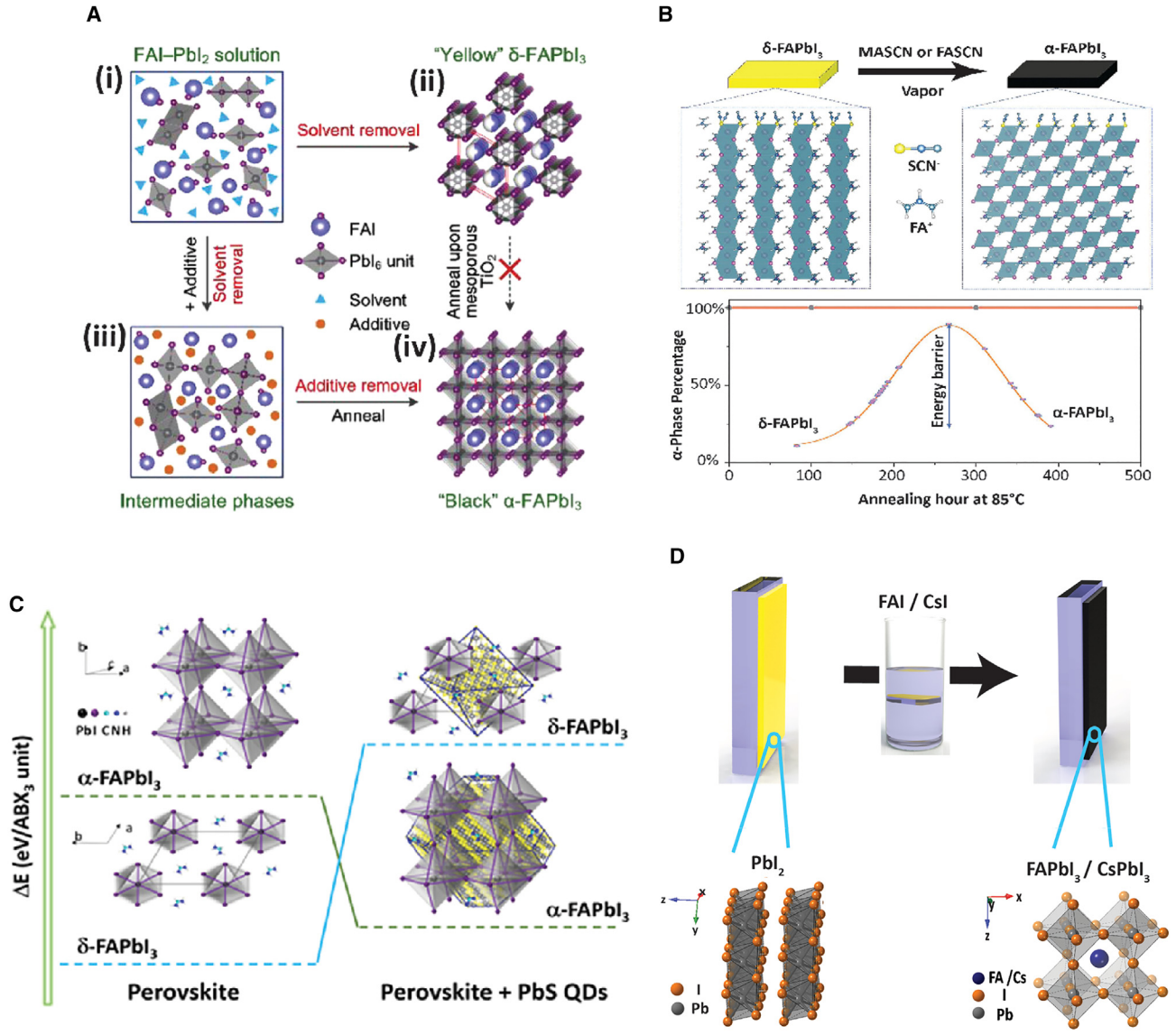

Figure 2. Formation of the metastable perovskite phases of $FAPbI_3$ and $CsPbI_3$

(A) Schematic illustration of $FAPbI_3$ phase evolution mechanism taking place through intermediate phases on mesoporous TiO_2 scaffolds. Reused from Wang et al.,[26] with permission, copyright ACS Publications (2015).

(B) Stable and phase-pure MASCN vapor-treated $FAPbI_3$ perovskite films. Reused from Lu et al.,[28] with permission, copyright AAAS (2021).

(C) Schematic illustration of PbS QD assisting in forming pure $FAPbI_3$ perovskite films. Reused from Masi et al.,[29] with permission, copyright ACS Publications (2020).

(D) Schematic illustration of formation of black $FAPbI_3$ and $CsPbI_3$ perovskite films by two-step method.

(3) The optimized MACl concentration is influenced by the pre-annealing doping formation energy of MACl into the α-phase $FAPbI_3$ perovskite structure and the post-annealing formation energy of the perovskite materials along with MAI.

Alkylammonium chlorides (RACl), such as propylamine hydrochloride (PACl) and butylamine hydrochloride (BACl) together with MACl, further lower the activation barrier and promote the formation of the pure black $FAPbI_3$ perovskite phase.[10] Dimethylammonium chloride (DMACl) is also employed as a crystallization agent to the

gradual transition via the 2D hexagonal face-sharing perovskite polytypes toward a 3D corner-sharing perovskite, resulting in highly crystalline and textured thin films with a face-up perovskite unit cell orientation.[31]

Moreover, a deposition technique utilizing MASCN or FASCN vapor treatment to convert δ-$FAPbI_3$ to the preferred pure α phase under the thermodynamic phase transition temperature (100°C) was reported.[28] In this study, a yellow δ-$FAPbI_3$ film was first obtained by conventional spin-coating method. The corresponding film was annealed at 100°C for 1 min and underwent MASCN vapor treatment for ~5 s until the color changed to black. In the reaction process, SCN^- anions can displace the iodides to form an intermediate phase with Pb^{2+} on the surface of δ-$FAPbI_3$ due to its strong affinity to Pb^{2+} ions. This gives rise to the rearrangement of ions at the surface of δ-$FAPbI_3$ and facilitates the phase transition to edge-sharing intermediates and further corner-sharing α-$FAPbI_3$ (Figure 2B).

For the formation of black $CsPbI_3$ perovskites, the addition of hydriodic acid (HI) in $CsPbI_3$-dimethylformamide (DMF) precursor solution or using the so-called hydrogen lead iodide ($HPbI_3$) as an alternative precursor to PbI_2 has been widely employed.[32,33] However, Kanatzidis and colleagues reported that HI can react with DMF to form dimethylammonium iodide (DMAI) and that the so-called $HPbI_3$ is in fact $DMAPbI_3$.[33] The exact composition of $CsPbI_3$ annealed at a temperature lower than 180°C is actually $Cs_{1-x}DMA_xPbI_3$. Since then, DMA^+ additive has been widely employed for preparing $CsPbI_3$ inorganic perovskite films. Based on the regulation of the CsI/$DMAPbI_3$ ratio in precursor solutions, high-quality $Cs_{1-x}DMA_xPbI_3$ ($0 \leq x \leq 1$) perovskite films can be prepared.[34] It has been reported that the concentration of DMAI in $CsPbI_3$ precursor solutions can determine the $CsPbI_3$ perovskite phase annealed at 210°C. $CsPbI_3$-DMAI and $CsPbI_3$-1.5DMAI lead to the formation of β-$CsPbI_3$ with an E_g of 1.68 eV, and γ-$CsPbI_3$ (E_g = 1.73 eV) can be obtained from $CsPbI_3$-0.5DMAI and $CsPbI_3$-0.75DMAI.[35,36] Based on choline iodide surface treatment, the β-$CsPbI_3$ film is constructed into PSCs with a PCE of 18.4%.[18] Pang et al. verified that $CsPbI_3$-DMAI film annealed at 180°C transforms into the thermodynamically stable $DMA_{0.15}Cs_{0.85}PbI_3$ (E_g = 1.67 eV) film with a small amount of Cs_4PbI_6 residue after 15 min. By extending the annealing time, $DMA_{0.15}Cs_{0.85}PbI_3$ film with Cs_4PbI_6 residue transforms into γ-$CsPbI_3$ film and then spontaneously converts to δ-$CsPbI_3$.[37] It is reported that a $CsPbI_3/Cs_{1-x}DMA_xPbI_3$ bulk heterojunction structure can be spontaneously formed, which facilitates the charge separation and collection process by enhancing the built-in potential. However, this is also detrimental to the carrier recombination loss and the increase of the open-circuit voltage.[38]

$CsPbI_3$ perovskite films with high crystallinity can also be obtained by adding DMAI and excess CsI in the perovskite precursor solution using the leaching method at RT. DMAI suppresses the generation of δ-$CsPbI_3$ at the initial stages of thin film formation, and an excess of CsI can compensate for the inevitable loss of CsI during the leaching treatment. A Cs-rich $Cs_{0.85}FA_{0.15}PbI_3$ perovskite film can be prepared by a Cs_4PbI_6-mediated synthesis method.[39] FAI-0.85CsI-PbI_2 precursor can form a 0D Cs_4PbI_6 and an FA-rich $FA_xCs_{1-x}PbI_3$ perovskite phase due to their lower free energy at low temperature. Cs_4PbI_6 with a low Cs cation diffusion barrier offers Cs^+ for the transformation of the FA-rich perovskite phase into the Cs-rich $FA_xCs_{1-x}PbI_3$ perovskite with the evaporation of FAI during annealing. The formation of Cs_4PbI_6 efficiently restrains the generation of the undesired δ-$CsPbI_3$ in the perovskite films.[40] MAI as an additive is also employed for the pure $CsPbI_3$ perovskite phase. A $MAPbI_3$-based perovskite template with excess CsI is firstly formed,

which transforms into pure γ-$CsPbI_3$ perovskite phase by the ion exchange of MA^+ with Cs^+ with the evaporation of MAI during annealing at 330°C.[41] It is also reported that annealing the precursor film with stoichiometric CsAc/MAI/PbI_2 (Ac:acetate) under the low crystallization temperature of 100°C for 2 min can form pure-phase black $CsPbI_3$ perovskite film.[42]

Strain engineering

Strain engineering is one of the key factors for the formation and stabilization of the pure perovskite phases of $FAPbI_3$ and $CsPbI_3$.

A strained epitaxial growth strategy of $FAPbI_3$ perovskite single-crystal thin films on lattice-mismatched halide perovskite $MAPbBr_{1.5}Cl_{1.5}$ substrates has been reported by Chen et al.[43] They described the effective modification of the crystal structure, reduction of band gap, and increase in hole mobility of the α-$FAPbI_3$ induced by strain. Strained epitaxy is also shown to have a substantial stabilization effect on the α-$FAPbI_3$ phase owing to the synergistic effect of epitaxial stabilization and strain neutralization. First, the interfacial energy of cubic α-$FAPbI_3$/cubic substrate is much lower than that of hexagonal δ-$FAPbI_3$/cubic substrate, which is the most critical factor for the formation and stabilization. The epitaxial lattice is constrained to the substrate owing to the strong ionic bonds between them and, therefore, the phase transition of the perovskite is restricted by the substrate lattice. Second, the driving force of the α-to-δ phase transition is believed to be the internal tensile strain in the α-$FAPbI_3$ unit cell, which can induce the formation of vacancies and subsequent phase transition. In this study, the epitaxial film is under compressive strain, which neutralizes the effect of the internal tensile strain. Therefore, the synergistic effect of the low-energy coherent epitaxial interface and the neutralizing compressive strain are the key to α-$FAPbI_3$ stabilization.[43] It is also reported that layered perovskites can template the solid-state phase conversion of $FAPbI_3$ from its hexagonal non-perovskite phase to the cubic perovskite phase, where the growth kinetics are controlled by a synergistic effect between strain and entropy.[44] In another example, PbS colloidal quantum dots (QDs) have been introduced into $FAPbI_3$ perovskite precursor solutions to form a stable perovskite $FAPbI_3$ black phase at low temperatures (Figure 2C). The surface chemistry of PbS plays a pivotal role due to the formation of strong bonds with the black phase but weak ones with the yellow phase.[29] PbS QDs with similar lattice parameters with inorganic perovskites have also been reported to transform and stabilize inorganic perovskite phases by lattice anchoring. The extent of improvement in film stability depends strongly on the lattice mismatch between QDs and perovskite. A lattice-matching QD/perovskite interface without strain is the most energetically favorable, and a certain amount of elastic strain can be accommodated without generating dislocations or defects.[45] $FAPbI_3$ and $CsPbI_3$ perovskite films can also be stabilized via the formation of substrate-clamping-driven texture with large biaxial strain at RT.[25,46]

Two-step method

Pure $FAPbI_3$ perovskite films cannot be formed by the one-step method based on pure $FAPbI_3$ precursor solution, especially on top of the mesoporous TiO_2 substrates.[25] The two-step method using dipping or spin-coating technology can avoid the formation of the yellow δ-$FAPbI_3$ phase for high-quality $FAPbI_3$ perovskite films (Figure 2D).[20,47] Recently, PSCs with a certified efficiency of 25.6% were obtained via the two-step method and RbCl addition.[48] Furthermore, efficiencies over 24% were obtained by applying an oriented nucleation mechanism for PSCs processed with the two-step method.[49] The critical point of this strategy is to avoid the presence

of undesirable phases during the nucleation process that takes place in the precursor solution, which can largely lead to the formation of high-quality pure black perovskite phase in the following crystallization process. High-quality $CsPbI_3$ perovskite films with Br^- and In^{3+} doping have been also fabricated by the dipping method.[50]

Progress and challenges of the formation of metastable black perovskite phase

Intermediate-phase engineering is a simple and effective way to develop metastable perovskite phases. Despite the tremendous progress that has been made, the understanding of the role and mechanisms for intermediate-phase engineering is still in its infancy.[27] The accurate crystal structures and compositions of the ABX_3-$A'X'$ intermediate phase have been rarely reported. Thus, it becomes difficult to accurately calculate the energy barrier values for the intermediate-to-perovskite phase formation. The choice of $A'X'$ additive is still empirical with insufficient mechanisms as guidance. The associated mechanisms deserve further exploration in combination with the information on their crystallization kinetics.

Strain promoting the formation of perovskite phase is also related to the decrease in formation energy barrier. The process is sometimes accompanied by the transition of the intermediate phase. For example, MASCN vapor facilitates the phase transition from δ-$FAPbI_3$ to edge-sharing intermediates and further corner-sharing α-$FAPbI_3$. The strain of formed pure α phase on the surface reduces the formation energy barrier from δ-$FAPbI_3$ to α-$FAPbI_3$ in the bulk and promotes the formation of a pure α-phase film.[11]

Currently, very few reports can be found discussing the role of the two-step method for the preparation of pure metastable perovskite phases. This has been observed even though it has been verified that the two-step method can promote the formation of $FAPbI_3$-based and $CsPbI_3$-based perovskite phases. We believe that the key point is to avoid the formation of the yellow δ-$FAPbI_3$ phase during the entire process. Together, the formation of the intermediate phases and strain engineering play important roles in the application of the two-step method, promoting the formation of metastable perovskite phases.

STABILIZATION OF $FAPbI_3$- AND $CsPbI_3$-BASED PEROVSKITE PHASES

Composition engineering

Composition engineering or element doping is an effective strategy to stabilize metastable $FAPbI_3$ and $CsPbI_3$ perovskite phase.

For $FAPbI_3$, it was reported that doping with MA^+, Cs^+, Rb^+, or Br^- can stabilize its perovskite phase.[9] For instance, incorporation of 15% $MAPbBr_3$ into $FAPbI_3$ results in the formation of stable $(FAPbI_3)_{0.85}(MAPbBr_3)_{0.15}$ perovskite phase.[7] It has been reported that asymmetric MA^+ exhibits a dipole moment ten times larger than symmetric FA^+, which can stabilize the 3D arrangement of the PbI_6 octahedra.[51] The stronger interaction between Br^- and surrounding ions compared to I^- also plays an important role in stabilizing the $FAPbI_3$-based perovskite phase.[52]

When 10% or 15% of $HC(NH_2)_2^+$ is replaced by Cs^+, photostability and moisture stability of perovskite film are significantly improved, which is attributed to the enhanced interaction between $HC(NH_2)_2^+$ and iodide due to contraction of cubo-octahedral volume.[53] Meanwhile, another explanation attributes Cs^+ stabilizing α-$FAPbI_3$ to the decrease of tolerance factor.[23] To further explain this phenomenon, the entropy and energy of related materials are calculated.[54] The δ phase of

$FAPbI_3$ consists of 1D pillars made of face-sharing PbI_6 octahedra. The δ-$CsPbI_3$ crystal is also made of 1D PbI_3 pillars surrounded by the cation, but these pillars consist of stacked and shifted edge-sharing PbI_6 octahedra. This also leads to the significant difference of the volume per stoichiometric unit. This suggests that the replacement of the organic cation FA^+ by the inorganic cation Cs^+ leads to a significant destabilization (an increase in energy) with respect to the two pure FA and/or $CsPbI_3$ δ phases, which is too large to be compensated by the mixing entropy. Thus, cation mixing cannot take place in the δ phase. On the contrary, the α- and β-$FAPbI_3$ perovskite phases are very similar to the perovskite phase of $CsPbI_3$, and the volume per stoichiometric unit of the three crystals is also comparable. The sum of the energy and mixing entropy contribution leads to a reduction of the free energy, resulting in stabilization of the mixed 3D perovskite over the δ phase. Replacement of iodide with a limited amount of bromide in mixed Cs/FA perovskites is thermodynamically favored (a decreasing energy) for perovskite phases.[54]

5% Rb^+ is also employed to dope $FAPbI_3$ perovskite phase for stable $Rb_{0.05}FA_{0.95}PbI_3$ perovskite films.[55,56] However, solid-state NMR shows that Rb^+ cannot enter into the $FAPbI_3$ perovskite lattice.[57] Thus far, the role of Rb doping in pure $FAPbI_3$ perovskites is still under debate. Triple-cation FAMACs-based perovskites and quadruple-cation FAMACsRb-based perovskites are also reported for stable perovskite phases.[58,59]

The low tolerance factor of $CsPbI_3$ (0.81) leads to a large lattice distortion, which is widely reported as the main reason for phase instability at RT.[23] Increasing the radius of A^+ ($r_A{}^+$), or reducing the $r_B{}^{2+}$ and $r_X{}^-$ in the ABX_3 crystal structure, will increase the relatively low tolerance factor of inorganic perovskites and, therefore, the phase stability.[17,60]

The smaller-size Br^- can substitute I^- in $CsPbI_3$ to form $CsPbI_{3-x}Br_x$ perovskites, which improves the stability of the black perovskite phase but also leads to an undesired blue shift of the absorption edge with an enlarged band gap for PSCs.[17]

Cs is the largest-size non-radioactive element in group IA of the periodic table, which indicates that no suitable monovalent inorganic cation (larger than Cs^+) is available for doping into the perovskite lattice, increasing the *t* of black-phase $CsPbI_3$. The larger-size organic cations FA^+ (r = 0.253 nm) and DMA^+ (r = 0.272 nm) can be incorporated into the perovskite lattice to form Cs-rich $Cs_{1-x}FA_xPbI_3$ and $Cs_{1-x}DMA_xPbI_3$, leading to an increase of tolerance factor and stability in comparison with $CsPbI_3$.[33,37,40]

Sn^{2+} (112 pm) with slightly smaller ionic radius compared to Pb^{2+} (119 pm) can substitute Pb^{2+} to form $CsPb_{1-x}Sn_xI_3$ alloys such as $CsPb_{0.6}Sn_{0.4}I_3$ (E_g = 1.38 eV), which can effectively increase tolerance factor and stability and adjust band gaps (Figures 3A and 3B).[61] $CsPb_{0.6}Sn_{0.4}I_3$ also shows superior stability in anti-oxidation compared to their hybrid counterparts. Cs^+ being smaller than MA^+ or FA^+ leads to stronger antibonding of Sn 5s with I 5p and smaller formation energy of Sn defects in inorganic perovskites.[61]

The incorporation of $EuCl_3$ into $CsPbI_3$ can stabilize the black phase under ambient conditions.[65] The smaller-size europium (Eu) can be doped into Pb-based inorganic perovskite lattice, which is verified by solid-state NMR and high-angle annular dark-field scanning transmission electron microscopy.[66] Mn^{2+} can be doped into $CsPbBr_3$

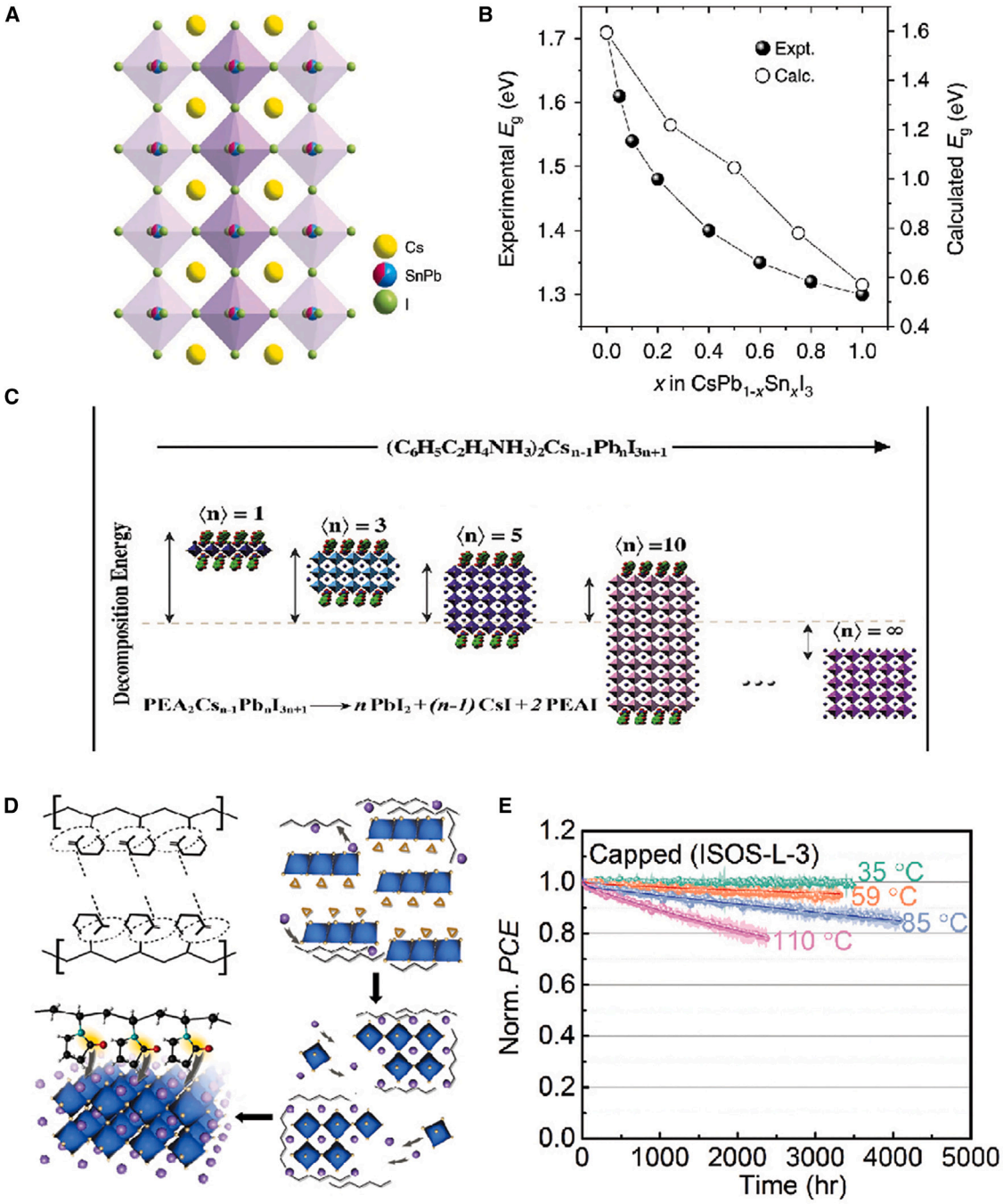

Figure 3. Stabilization of the metastable perovskite phases of $FAPbI_3$ and $CsPbI_3$

(A) Schematic crystal structure of $CsPb_{1-x}Sn_xI_3$.

(B) Variation of experimental (solid circles) and calculated (open circles) E_g as a function of x in $CsPb_{1-x}Sn_xI_3$. (A) and (B) are adapted from Hu et al.[61] Reused with permission, copyright 2020, Springer Nature.

(C) $PEA_2Cs_{n-1}PbnX_{3n+1}$'s unit cell structure and disintegration energetics via first-principles density functional theory of perovskite with various n values. Reused from Jiang et al.,[62] with permission, copyright 2018, Elsevier.

(D) The PVP-induced $CsPbI_3$ cubic phase stability mechanism. Reused from Li et al.,[63] with permission, copyright 2018, Springer Nature.

(E) Standard deviation envelopes and operation stability for capped $CsPbI_3$ PSCs operating at 35°C, 59°C, 85°C, and 110°C. Reused from Zhao et al.,[64] with permission, copyright 2022, AAAS.

and $CsPbCl_3$ perovskite lattice up to at least 8 mol % and 3 mol %, respectively.[67] The incorporation of Mn^{2+} also stabilizes the black phase of $CsPbI_3$ nanocrystals, which promotes the improvement of PCE of solar cells.[68,69] Aliovalent Bi^{3+} can be incorporated into $CsPbI_3$ lattice, reducing the band gap and improving the phase stability.[70] Sb^{3+} incorporated in $CsPbI_3$ also increases the phase stability of the films.[71] More examples of the effect of B-site doping in all-inorganic $CsPbI_3$-based absorbers on the performance and stability of perovskite photovoltaics can be found in a more detailed review.[72]

Dimensional engineering

It is widely reported that reducing perovskite dimension to form 2D (or quasi-2D) perovskites or perovskite nanocrystal can improve the perovskite phase stability of $FAPbI_3$ and $CsPbI_3$.

Incorporating 2D perovskites such as phenylethylammonium lead iodide (PEA_2PbI_4) can fabricate phase-pure $FAPbI_3$ with high optoelectronic quality and stability, due to the large PEA molecules from 2D perovskite precursors interacting with $FAPbI_3$ crystals, and suppresses the formation of δ phase.[73] During the process, there is spontaneous formation of 2D perovskite at the grain boundaries of $FAPbI_3$ film, suppressing moisture attack and ionic transport, giving rise to an improved stability of the α-$FAPbI_3$. It is also reported that the surrounding PEA^+ ions act as molecular locks to strengthen $FAPbI_3$ domains and passivate the surface defects, leading to improved phase stability.[74] Long-chain alkylammonium bromides have been widely and commonly adapted for defect passivation and stabilization of $FAPbI_3$-based PSCs, and the mechanism behind this is closely related to the formation of stable low-dimension perovskites via the reaction with surface excess PbI_2.[75–77] In addition, 2D/3D heterojunction engineering at the buried interface was realized by incorporating a small amount of 2-aminoindan hydrochloride toward high-performance inverted methylammonium-free PSCs.[78] One has to note that although 2D engineering can improve the phase stability of metastable $FAPbI_3$, it does not guarantee the device stability under heat and light. Recent findings have proved that the surface 2D perovskite cations tend to diffuse into the bulk of 3D perovskite, causing the deterioration of the 2D/3D interface and decline of performance of the solar cells. In light of this, a crosslinked polymer into the interface or non-reactive ammonium ligand intercalation was employed to inhibit the ion diffusion and improve the long-term operational stability.[79,80] Besides, the introduction of 2D perovskite into $CsPbI_3$ leads to the formation of $BA_2CsPb_2I_7$ and $PEA_2Cs_{n-1}Pb_nI_{3n+1}$ ($1 \leq n \leq \infty$) quasi-2D perovskites or the $CsPbI_3 \cdot 0.025EDAPbI_4$ perovskite, increasing phase stability against humidity and heat (Figure 3C).[55,62,81]

While bulk $CsPbI_3$ can easily transform into the yellow phase in ambient conditions, black-phase $FAPbI_3$ and $CsPbI_3$ nanocrystals have been reported to be stable due to the contribution of surface energies.[82] For nanocrystals of $CsPbI_3$ with diameters larger than 5.6 nm, the formation of δ-$CsPbI_3$ is favored, while for diameters smaller than 5.6 nm, the γ-$CsPbI_3$ phase is energetically more stable than the δ-yellow phase. Decreasing the diameter below 3.7 nm, α-$CsPbI_3$ becomes thermodynamically stable.[83]

Additive engineering

Additive engineering is a technique employed to stabilize $FAPbI_3$-based and $CsPbI_3$-based perovskite phases by enhancing the activation energy barrier or protect perovskite films from moisture attack.[52]

Organic ammonium salts such as benzylammonium (Bz) iodide are introduced into $FAPbI_3$ precursor solutions. The BzI can interact with α-$FAPbI_3$ at the atomic level through hydrogen bonding, stabilizing it against the detrimental α-to-δ phase transition.[84] 1-Hexyl-3-methylimidazolium iodide ionic liquid was employed as an additive to stabilize $FAPbI_3$ perovskite due to grain coarsening caused by the decrease in activation energy of the grain boundary migration.[85] Methylenediammonium dichloride ($MDACl_2$), with a slightly larger cation, creates a stronger hydrogen bond between MDA^{2+} and perovskite lattice, leading to a structurally stabilized α-$FAPbI_3$.[86] Recently, anion-π interactions by an additive of hexafluorobenzene were introduced to suppress phase impurities in $FAPbI_3$ for highly efficient and stable PSCs.[87] Furthermore, for $FA_{1-x}Cs_xPbI_3$ ($x \leq 0.1$) perovskite, the phase stability is closely related to the homogeneity of cation distribution in-plane and out-of-plane of the absorber, which can be enhanced by the addition of selenophene and 1-(phenylsulfonyl)pyrrole, respectively, leading to better performance with efficiency and stability of devices.[88,89]

Oleylammonium and phenylethylammonium additives introduced into inorganic perovskite precursor solution led to the formation of metastable α- and β-$CsPbI_3$ films, respectively. These ligands can prevent grain aggregation and growth, preventing the interaction of moisture with the perovskite films. Both black-phase films were able to remain stable for more than 4 months under ambient conditions.[90]

Polyvinylpyrrolidone (PVP) introduced into $CsPbI_3$ precursor solution forms extra-long-term stable $CsPbI_3$ perovskite film. The acylamino groups of PVP increase electron cloud density on the surface of $CsPbI_3$, which lowers surface energy and stabilizes α-$CsPbI_3$ (Figure 3D).[63] Furthermore, a small quantity of poly(ethylene oxide) (PEO) introduced into the $CsPbI_3$ precursor solution effectively promotes the formation of the black phase at a low crystallization temperature, reduces the grain size during crystallization, and enhances the phase stability of the $CsPbI_3$ perovskite film. PEO coordinates with the ionic surfaces of the $CsPbI_3$ grains during crystal impingement and passivates the grain boundaries in the intragrain regions.[91]

Adding sulfobetaine zwitterion into the precursor solution impedes crystallization and leads to the formation of $CsPbI_3$ perovskite film, with average grain size of 30 nm, via electrostatic interactions between the zwitterion and the PbI_2-DMSO colloids in the precursor solution.[92]

Surface engineering

Organic molecules have been applied to improve the stability of perovskite thin films by forming a stable surface layer, reducing surface energy, or passivating the defects on $FAPbI_3$-based or $CsPbI_3$-based perovskite surfaces.

Surface functionalization can enable the stabilization of the metastable perovskite phase in pure $FAPbI_3$ without cation or anion alloying. The long-chain alkyl or aromatic ammonium cations bind to the surface of perovskite structure and reduce the surface energy, which plays a dominant role in stabilizing the metastable perovskite phase.[93] An ultrathin and highly uniform 2D $(FEA)_2PbI_4$ (FEA, pentafluorophenylethylammonium) layer on the 3D $FAPbI_3$-based perovskite layers is prepared by absorbing the non-perovskite phase of $FAPbI_3$ present at the surface of 3D perovskite layer, via the reaction $FAPbI_3(\delta) + 2FEAI = (FEAI)_2PbI_4 + FAI$. When combined with the hydrophobicity of $(FEA)_2PbI_4$, the resulting non-encapsulated PSC achieved

outstanding operational stability at the maximum power point under 1 sun irradiation in ambient conditions (40% relative humidity).[94]

PEAI forms a defect-passivating organic cation terminated surface on a $CsPbI_3$ film that improves phase stability and moisture resistance.[95] Phenyltrimethylammonium bromide (PTABr) leads to simultaneous gradient Br doping and surface passivation of organic PTA cation, which enhance the phase stability of $CsPbI_3$.[96] The application of a stable $CsPbI_3$ QD film can be employed as a surface layer to protect the black perovskite phase $CsPbI_{2+x}Br_{1-x}$ of a graded band gap, and achieves proper band-edge bending for improved carrier collection.[97] Combining the $CsPbI_3$ QD as the absorbing layer and the CuSCN inorganic hole transport layer, all-inorganic PSCs with a 2D inorganic perovskite modified layer achieve an excellent operating stability, with T_{80} > 2,100 h at 110°C under constant illumination. The latter corresponds to an extrapolated T_{80} of more than 5 years at 35°C (where T_{80} is the time taken for device efficiency to be reduced to 80% of its initial value) (Figure 3E).[64]

Progress and challenges of the stabilization of metastable black perovskite phase

For stabilizing metastable perovskite phases, composition engineering is nowadays the most effective method. Modifying the tolerance factor is widely considered a key factor. It is usually considered that decreasing the tolerance factor is beneficial for stabilizing $FAPbI_3$ perovskite phase with a large tolerance factor (0.987), and increasing the tolerance factor is conducive to stabilizing $CsPbI_3$ perovskite phase with a low value (0.81). However, this cannot explain why Br doping stabilizes the $FAPbI_3$ perovskites, since Br leads to an increase in tolerance factor.[7,16,98] Another observation suggests that the contraction of the cubo-octahedral volume stabilizes the perovskite phase. This is difficult to reconcile with the observation that Rb^+ (smaller ion radius than Cs^+) lattice doping in inorganic perovskites leads to increasing phase instability.[99,100] Entropy or free energy can explain some phenomena of Cs lattice doping in $FAPbI_3$ increasing phase stability,[15,54,101] but the theory is still in its infancy. As element lattice doping leads to changes of intrinsic material properties, composition engineering is expected to reduce the Gibbs free energy (process II in Figure 1E) of perovskites themselves and increase the energy barrier (process III in Figure 1E) from perovskite phases to non-perovskite phases for stabilizing perovskite phases. As phase transformation between black perovskites and yellow non-perovskites is determined by the competitive relationship of their thermodynamic stability, the role of the doping element in the yellow non-perovskite phases has to be studied further to explore the mechanisms of metastable perovskite phase stabilization.

Dimensional engineering, additive engineering, and surface engineering are mainly expected to modify the surface energy, reducing defects and adjusting strain to increase the energy barrier (process III in Figure 1E) from the perovskite phases to non-perovskite phases. Further increasing the stability of grain boundary and surface is the key to large-area solar panels.[79,102]

CONCLUSIONS AND OUTLOOK

Summary of thermodynamic process

Figure 4 summarizes the thermodynamic process for the formation and stabilization of $FAPbI_3$-based and $CsPbI_3$-based metastable perovskites. Intermediate-phase engineering and the two-step method promote the formation of $FAPbI_3$-based and $CsPbI_3$-based metastable perovskites by reducing the formation energy barrier. Composition engineering can reduce the Gibbs free energy of perovskite

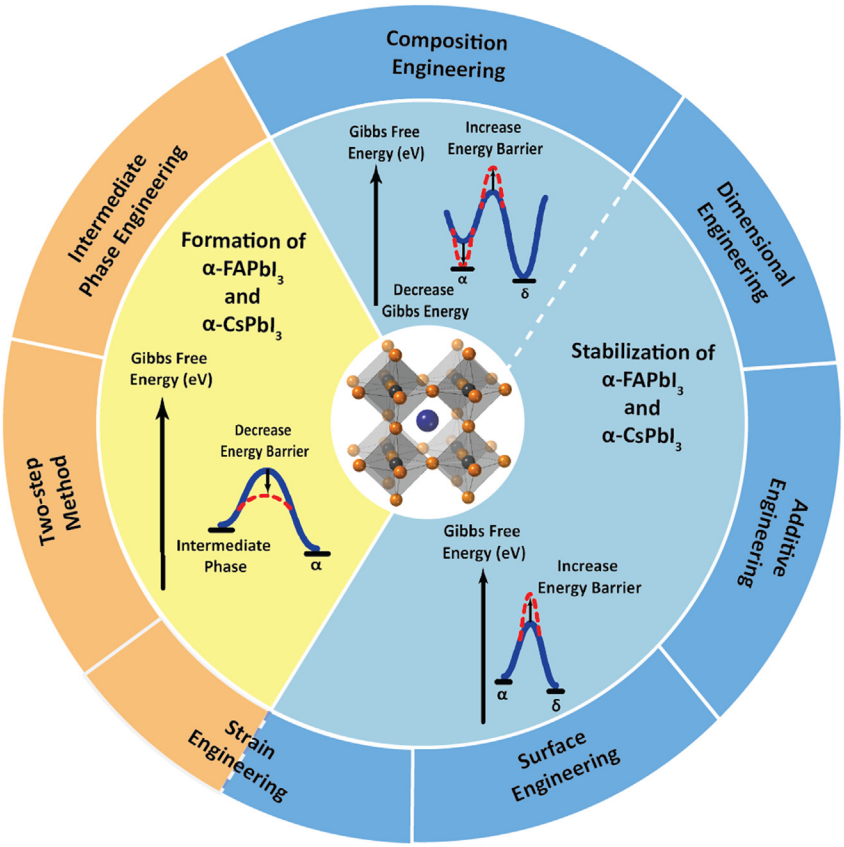

Figure 4. Summary of the thermodynamic process of Gibbs free energy change and energy barrier are presented qualitatively for the formation and stabilization of $FAPbI_3$-based and $CsPbI_3$-based metastable perovskites, applying various strategies

materials and increase the energy barrier from perovskite phases to yellow non-perovskite phases. The latter is one of the most effective strategies to stabilize the metastable perovskite phases. It is also an important strategy for the formation of pure metastable perovskite phases as the Gibbs free energy decreases. Other widely reported strategies to stabilize the perovskite phases include dimensional engineering, additive engineering, and surface engineering, which mainly increase the energy barrier from perovskite phases to the non-perovskite phases. Strain engineering can not only promote the formation of metastable perovskites by reducing the formation energy barrier but also suppress the transition from perovskite phases to yellow non-perovskite phases by increasing their energy barrier. Strain engineering can also accompany the other aforementioned strategies.

Above all, for the formation of metastable black perovskite phase, the critical point is to avoid the formation of the stable non-perovskite phase during crystal nucleation and growth from the beginning. Once the stable yellow phase is formed, it will be very difficult to fully convert it into metastable black phase during the subsequent annealing process. This is due to the non-equilibrium thermal condition applied (annealing time is limited to tens of minutes to less than 1 h) and gradient heating starting from the bottom to the top of the thin film using a hotplate.[103] When a non-uniform film is formed under thermal treatment, the non-perovskite phase will remain after cooling down. This point of view is also true for other photovoltaic materials with multi-element composition, e.g., kesterite $Cu_2ZnSn(S,Se)_4$ (CZTSSe).

Thermodynamically, kesterite has a very narrow single-phase zone in the phase diagram, which promotes the formation of secondary phases such as binary and ternary phases in the absorber films. Thus, a pure kesterite phase is usually difficult to achieve. The world record efficiency remained below 13% for more than 5 years until a recent breakthrough achieves almost 15%, due to thermodynamic control of the crystal growth to form a kesterite phase directly and avoid the formation of secondary phases from the beginning.[12,104] The lesson learned here may provide enlightenment for other metastable semiconductors.

For the stabilization of the metastable perovskite phase, the strategies are mainly kinetic: extremely increase the transition energy barrier from metastable phase to stable phase in order to vastly slow down the conversion rate from the metastable phase to stable phase. The example is ready-made: glass. It is well known that glass is amorphous material, and it is metastable at RT. Given the super-high conversion energy barrier from amorphous glass to crystal, glass needs hundreds or even thousands of years to convert into crystal and lose uniform transparency, and thus we can use it as a stable material for tens of years. Therefore, it is possible that PSCs following the same strategy can overcome the metastability issues and match the benchmark of commercial standards of 25 years.

Multiple-junction application of metastable perovskites

Multijunction solar cells offer routes to increase PCE, which can extend beyond the S-Q efficiency limit of single-junction photovoltaics.[105,106] $CsPbI_3$- and $FAPbI_3$-based perovskites show potential application in multiple junctions.[107,108] $FAPbI_3$-based perovskites can be employed in middle subcells in perovskite/perovskite/Si triple-junction solar cells.[107,109,110] The band gap (~1.5 eV) of $FAPbI_3$ perovskite films is still too large compared to the ideal band gap (~1.45 eV) in middle subcells.[111,112] The $FAPbI_3$ single-crystal film with ~1.43 eV band gap shows great potential for its application as the photosensitive layer in the middle subcell.[20,113] There are still many challenges to overcome for the preparation of high-quality perovskite crystal films on industry-relevant textured crystalline silicon solar cells. $CsPbI_3$-based perovskites with ~1.7 eV band gap are ideal candidates for perovskite/Si tandem solar cells, which deliver good light and thermal stability.[14,23,24] The low-temperature fabrication of high-quality and thick $CsPbI_3$-based perovskite films on textured crystalline silicon is still an important challenge to overcome before achieving highly efficient $CsPbI_3$ perovskite/Si tandem solar cells.[39,108] Intermediate-phase engineering and strain engineering are the candidate strategies for overcoming these challenges.

Innovative application of the metastable perovskites

Even though the reserve transition between black perovskite phases and yellow non-perovskite phases is detrimental to long-term stability of photovoltaic devices, metastable perovskites can be employed in smart photovoltaic windows and sensors as stimuli-responsive materials.[114,115] Smart photovoltaic windows represent a promising green technology to harvest solar energy as well as controlling the amount of incoming light into buildings. Inorganic halide perovskite cesium lead iodide/bromide with reversible phase transition between the photoactive perovskite and transparent non-perovskite phases has been employed in smart photovoltaic window applications. The solar cell showed PCE of 4.69% versus 0.15% and visible transparency of 35.4% versus 81.7% in its perovskite and non-perovskite states, respectively. Over 85% of its peak PCE was retained after 40 switching cycles. However, switching between the states involved high-temperature annealing (>100°C) and was relatively slow, taking up to several hours. To decrease the transition

temperature and achieve a quick transition rate, decreasing the energy barrier between black perovskite phases and yellow non-perovskite phases is necessary, which is different from that in photovoltaic applications.

Scalable fabrication and commercial viability of metastable perovskites

Even though a wide variety of approaches has been studied to resolve the phase stability of metastable perovskites in laboratory-scale cells, these issues should still be noted when processing techniques are employed in industrially upscaled modules. The scalable fabrication of perovskite films mainly includes scalable solution-deposition methods such as blade coating, slot-die coating, meniscus coating, spray coating, inkjet printing, screen printing, and electrodeposition and vapor-phase deposition such as vacuum-evaporated deposition and chemical vapor deposition.[116] The crystallization process of scalable fabrication is often different from that of laboratory fabrication, and the former has a larger challenge in uniformly coating a compact perovskite absorber with photoactive phases. It is thus important to assess the impact of scalable processes on pure perovskite phase and film quality of these metastable perovskite films together. In scalable solution deposition, a longer process window than that in laboratory fabrication is necessary, and the formation of the pure intermediate phase is beneficial for increasing the quality of perovskite films.[27,116] Thus, a relatively stable intermediate phase before annealing should be beneficial for improving the performance and repeatability of perovskite modules. Compared to scalable solution-deposition methods, vapor-phase deposition is a high-throughput fabrication technique because of its solvent-free characteristic, precise control of film thickness, and compatibility with large-scale production. To date, the efficiency and working lifetimes of minimodules manufactured by vapor-phase deposition still lag far behind solution-deposition processed photovoltaics, mainly due to the defects caused by phase impurities, element non-uniform distribution, and non-stoichiometry.[117,118] A recently reported intermediate-phase process with integrated Cl facilitates perovskite phase transition from the δ phase to the α phase and increases the crystallinity of the resulting perovskite nanocrystals, leading to a high-quality film with fewer defects.[117] Besides, the hybrid processing technique that combines scalable solution deposition and vapor-phase deposition allows modules to have an obvious improvement in efficiency and stability.[119] Overall, the formation and stabilization of the metastable perovskite phase should demand more attention in upscaling fabrication to accelerate the commercial application of perovskite photovoltaics.

ACKNOWLEDGMENTS

H.X. thanks the start-up fund of Pengcheng Peacock Project and the start-up fund of Shenzhen University (no. 000002112129). M.L. gives thanks to the Spanish State Research Agency for the grant Self-Power (PID2019-104272RB-C54/AEI/10.13039/501100011033). The ICN2 is supported by the Severo Ochoa Centres of Excellence Programme, grant CEX2021-001214-S, funded by MCIN/AEI/10.13039.501100011033.

AUTHOR CONTRIBUTIONS

H.X. directed the project. H.X. and S.H. conceived the idea. S.H. and A.R.T. prepared the draft. M.L.-C. corrected the manuscript. S.H., A.R.T., X.Z., S.P., M.L.-C., and H.X. participated in the discussion and revision of the manuscript.

DECLARATION OF INTERESTS

M.L.-C. is on the Advisory Board of *Cell Reports Physical Science*.

REFERENCES

1. Kojima, A., Teshima, K., Shirai, Y., and Miyasaka, T. (2009). Organometal halide perovskites as visible-light sensitizers for photovoltaic cells. J. Am. Chem. Soc. *131*, 6050–6051. https://doi.org/10.1021/Ja809598r.

2. Stoumpos, C.C., Malliakas, C.D., and Kanatzidis, M.G. (2013). Semiconducting tin and lead iodide perovskites with organic cations: Phase transitions, high mobilities, and near-infrared photoluminescent properties. Inorg. Chem. *52*, 9019–9038. https://doi.org/10.1021/Ic401215x.

3. Lee, M.M., Teuscher, J., Miyasaka, T., Murakami, T.N., and Snaith, H.J. (2012). Efficient hybrid solar cells based on meso-superstructured organometal halide perovskites. Science *338*, 643–647. https://doi.org/10.1126/science.1228604.

4. Chen, Q., Wu, J., Ou, X., Huang, B., Almutlaq, J., Zhumekenov, A.A., Guan, X., Han, S., Liang, L., Yi, Z., et al. (2018). All-inorganic perovskite nanocrystal scintillators. Nature *561*, 88–93. https://doi.org/10.1038/s41586-018-0451-1.

5. Lin, K., Xing, J., Quan, L.N., de Arquer, F.P.G., Gong, X., Lu, J., Xie, L., Zhao, W., Zhang, D., Yan, C., et al. (2018). Perovskite light-emitting diodes with external quantum efficiency exceeding 20 per cent. Nature *562*, 245–248. https://doi.org/10.1038/s41586-018-0575-3.

6. Kim, H.-S., Lee, C.-R., Im, J.-H., Lee, K.-B., Moehl, T., Marchioro, A., Moon, S.-J., Humphry-Baker, R., Yum, J.-H., Moser, J.E., et al. (2012). Lead Iodide Perovskite Sensitized All-Solid-State Submicron Thin Film Mesoscopic Solar Cell with Efficiency Exceeding 9. Sci. Rep. *2*, 591. https://doi.org/10.1038/srep00591.

7. Jeon, N.J., Noh, J.H., Yang, W.S., Kim, Y.C., Ryu, S., Seo, J., and Seok, S.I. (2015). Compositional engineering of perovskite materials for high-performance solar cells. Nature *517*, 476–480. https://doi.org/10.1038/nature14133.

8. Min, H., Lee, D.Y., Kim, J., Kim, G., Lee, K.S., Kim, J., Paik, M.J., Kim, Y.K., Kim, K.S., Kim, M.G., et al. (2021). Perovskite solar cells with atomically coherent interlayers on SnO_2 electrodes. Nature *598*, 444–450. https://doi.org/10.1038/s41586-021-03964-8.

9. Liu, X., Luo, D., Lu, Z.-H., Yun, J.S., Saliba, M., Seok, S.I., and Zhang, W. (2023). Stabilization of photoactive phases for perovskite photovoltaics. Nat. Rev. Chem *7*, 462–479. https://doi.org/10.1038/s41570-023-00492-z.

10. Park, J., Kim, J., Yun, H.S., Paik, M.J., Noh, E., Mun, H.J., Kim, M.G., Shin, T.J., and Seok, S.I. (2023). Controlled growth of perovskite layers with volatile alkylammonium chlorides. Nature *616*, 724–730. https://doi.org/10.1038/s41586-023-05825-y.

11. Lu, H., Liu, Y., Ahlawat, P., Mishra, A., Tress, W.R., Eickemeyer, F.T., Yang, Y., Fu, F., Wang, Z., Avalos, C.E., et al. (2020). Vapor-assisted deposition of highly efficient, stable black-phase FAPbI3 perovskite solar cells. Science *370*. https://doi.org/10.1126/science.abb8985.

12. National Renewable Energy Laboratory (NREL) (2024). Best Research-Cell Efficiency Chart.

13. Chu, X., Ye, Q., Wang, Z., Zhang, C., Ma, F., Qu, Z., Zhao, Y., Yin, Z., Deng, H.-X., Zhang, X., and You, J. (2023). Surface in situ reconstruction of inorganic perovskite films enabling long carrier lifetimes and solar cells with 21% efficiency. Nat. Energy *8*, 372–380. https://doi.org/10.1038/s41560-023-01220-z.

14. Ahmad, W., Khan, J., Niu, G., and Tang, J. (2017). Inorganic $CsPbI_3$ Perovskite-Based Solar Cells: A Choice for a Tandem Device. Sol. RRL *1*, 1700048. https://doi.org/10.1002/solr.201700048.

15. Chen, T., Foley, B.J., Park, C., Brown, C.M., Harriger, L.W., Lee, J., Ruff, J., Yoon, M., Choi, J.J., and Lee, S.-H. (2016). Entropy-driven structural transition and kinetic trapping in formamidinium lead iodide perovskite. Sci. Adv. *2*, e1601650. https://doi.org/10.1126/sciadv.1601650.

16. Marronnier, A., Roma, G., Boyer-Richard, S., Pedesseau, L., Jancu, J.M., Bonnassieux, Y., Katan, C., Stoumpos, C.C., Kanatzidis, M.G., and Even, J. (2018). Anharmonicity and disorder in the black phases of cesium lead iodide used for stable inorganic perovskite solar cells. ACS Nano *12*, 3477–3486. https://doi.org/10.1021/acsnano.8b00267.

17. Wang, Z., Zhang, J., Guo, W., Xiang, W., and Hagfeldt, A. (2021). Formation and stabilization of inorganic halide perovskites for photovoltaics. Matter *4*, 528–551. https://doi.org/10.1016/j.matt.2020.12.007.

18. Wang, Y., Dar, M.I., Ono, L.K., Zhang, T., Kan, M., Li, Y., Zhang, L., Wang, X., Yang, Y., Gao, X., et al. (2019). Thermodynamically stabilized β-$CsPbI_3$–based perovskite solar cells with efficiencies >18. Science (New York, N.Y.) *365*, 591–595. https://doi.org/10.1126/science.aav8680.

19. Eperon, G.E., Stranks, S.D., Menelaou, C., Johnston, M.B., Herz, L.M., and Snaith, H.J. (2014). Formamidinium lead trihalide: a broadly tunable perovskite for efficient planar heterojunction solar cells. Energy Environ. Sci. *7*, 982–988. https://doi.org/10.1039/C3ee43822h.

20. Pang, S., Hu, H., Zhang, J., Lv, S., Yu, Y., Wei, F., Qin, T., Xu, H., Liu, Z., and Cui, G. (2014). $NH_2CH{=}NH_2PbI_3$: An Alternative Organolead Iodide Perovskite Sensitizer for Mesoscopic Solar Cells. Chem. Mater. *26*, 1485–1491. https://doi.org/10.1021/cm404006p.

21. Shockley, W., and Queisser, H.J. (1961). Detailed balance limit of efficiency of p-n junction solar cells. J. Appl. Phys. *32*, 510–519. https://doi.org/10.1063/1.1736034.

22. Stoumpos, C.C., and Kanatzidis, M.G. (2015). The renaissance of halide perovskites and their evolution as emerging semiconductors. Acc. Chem. Res. *48*, 2791–2802. https://doi.org/10.1021/acs.accounts.5b00229.

23. Li, Z., Yang, M., Park, J.-S., Wei, S.-H., Berry, J.J., and Zhu, K. (2015). Stabilizing Perovskite Structures by Tuning Tolerance Factor: Formation of Formamidinium and Cesium Lead Iodide Solid-State Alloys. Chem. Mater. *28*, 284–292. https://doi.org/10.1021/acs.chemmater.5b04107.

24. Zhou, Y., and Zhao, Y. (2019). Chemical stability and instability of inorganic halide perovskites. Energy Environ. Sci. *12*, 1495–1511. https://doi.org/10.1039/C8EE03559H.

25. Zhou, Y., Kwun, J., Garces, H.F., Pang, S., and Padture, N.P. (2016). Observation of phase-retention behavior of the HC(NH2)2PbI3 black perovskite polymorph upon mesoporous TiO2 scaffolds. Chem. Commun. *52*, 7273–7275. https://doi.org/10.1039/c6cc02086k.

26. Wang, Z., Zhou, Y., Pang, S., Xiao, Z., Zhang, J., Chai, W., Xu, H., Liu, Z., Padture, N.P., and Cui, G. (2015). Additive-Modulated Evolution of $HC(NH_2)_2PbI_3$ Black Polymorph for Mesoscopic Perovskite Solar Cells. Chem. Mater. *27*, 7149–7155. https://doi.org/10.1021/acs.chemmater.5b03169.

27. Xiang, W., Zhang, J., Liu, S.F., Albrecht, S., Hagfeldt, A., and Wang, Z. (2022). Intermediate phase engineering of halide perovskites for photovoltaics. Joule *6*, 315–339. https://doi.org/10.1016/j.joule.2021.11.013.

28. Lu, H., Liu, Y., Ahlawat, P., Mishra, A., Tress, W.R., Eickemeyer, F.T., Yang, Y., Fu, F., Wang, Z., Avalos, C.E., et al. (2020). Vapor-assisted deposition of highly efficient, stable black-phase $FAPbI_3$ perovskite solar cells. Science *370*, eabb8985. https://doi.org/10.1126/science.abb8985.

29. Masi, S., Echeverría-Arrondo, C., Salim, K.M.M., Ngo, T.T., Mendez, P.F., López-Fraguas, E., Macias-Pinilla, D.F., Planelles, J., Climente, J.I., and Mora-Seró, I. (2020). Chemi-Structural Stabilization of Formamidinium Lead Iodide Perovskite by Using Embedded Quantum Dots. ACS Energy Lett. *5*, 418–427. https://doi.org/10.1021/acsenergylett.9b02450.

30. Kim, M., Kim, G.-H., Lee, T.K., Choi, I.W., Choi, H.W., Jo, Y., Yoon, Y.J., Kim, J.W., Lee, J., Huh, D., et al. (2019). Methylammonium chloride induces intermediate phase stabilization for efficient perovskite solar cells. Joule *3*, 2179–2192. https://doi.org/10.1016/j.joule.2019.06.014.

31. McMeekin, D.P., Holzhey, P., Fürer, S.O., Harvey, S.P., Schelhas, L.T., Ball, J.M., Mahesh, S., Seo, S., Hawkins, N., Lu, J., et al. (2023). Intermediate-phase engineering via dimethylammonium cation additive for stable perovskite solar cells. Nat. Mater. *22*, 73–83. https://doi.org/10.1038/s41563-022-01399-8.

32. Eperon, G.E., Paternò, G.M., Sutton, R.J., Zampetti, A., Haghighirad, A.A., Cacialli, F., and Snaith, H.J. (2015). Inorganic caesium lead iodide perovskite solar cells. J. Mater. Chem. A Mater. *3*, 19688–19695. https://doi.org/10.1039/C5TA06398A.

33. Ke, W., Spanopoulos, I., Stoumpos, C.C., and Kanatzidis, M.G. (2018). Myths and reality of $HPbI_3$ in halide perovskite solar cells. Nat. Commun. *9*, 4785. https://doi.org/10.1038/s41467-018-07204-y.

34. Pei, Y., Liu, Y., Li, F., Bai, S., Jian, X., and Liu, M. (2019). Unveiling property of hydrolysis-derived $DMAPbI_3$ for perovskite devices: Composition engineering, defect mitigation, and stability optimization. iScience *15*, 165–172. https://doi.org/10.1016/j.isci.2019.04.024.

35. Wang, Y., Liu, X., Zhang, T., Wang, X., Kan, M., Shi, J., and Zhao, Y. (2019). The role of dimethylammonium iodide in $CsPbI_3$ perovskite fabrication: Additive or dopant? Angew. Chem. Int. Ed. *58*, 16691–16696. https://doi.org/10.1002/anie.201910800.

36. Wang, Y., Liu, X., Zhang, T., Wang, X., Kan, M., Shi, J., and Zhao, Y. (2019). The Role of Dimethylammonium Iodide in $CsPbI_3$ Perovskite Fabrication: Additive or Dopant? Angew. Chem., Int. Ed. Engl. *58*, 16691–16696. https://doi.org/10.1002/anie.201910800.

37. Meng, H., Shao, Z., Wang, L., Li, Z., Liu, R., Fan, Y., Cui, G., and Pang, S. (2019). Chemical composition and phase evolution in DMAI-derived inorganic perovskite solar cells. ACS Energy Lett. *5*, 263–270. https://doi.org/10.1021/acsenergylett.9b02272.

38. Sun, X., Shao, Z., Li, Z., Liu, D., Gao, C., Chen, C., Zhang, B., Hao, L., Zhao, Q., Li, Y., et al. (2022). Highly efficient $CsPbI_3/Cs_{1-x}DMA_xPbI_3$ bulk heterojunction perovskite solar cell. Joule *6*, 850–860. https://doi.org/10.1016/j.joule.2022.02.004.

39. Sun, X., Shao, Z., Rao, Y., Meng, H., Gao, C., Chen, C., Liu, D., Lv, P., Li, Z., Wang, X., et al. (2020). A Low-Temperature Additive-Involved Leaching Method for Highly Efficient Inorganic Perovskite Solar Cells. Adv. Energy Mater. *11*, 2002754. https://doi.org/10.1002/aenm.202002754.

40. Shao, Z., Meng, H., Du, X., Sun, X., Lv, P., Gao, C., Rao, Y., Chen, C., Li, Z., Wang, X., et al. (2020). Cs_4PbI_6 -Mediated Synthesis of Thermodynamically Stable $FA_{0.15}Cs_{0.85}PbI_3$ Perovskite Solar Cells. Adv. Mater. *32*, e2001054. https://doi.org/10.1002/adma.202001054.

41. Lau, C.F.J., Wang, Z., Sakai, N., Zheng, J., Liao, C.H., Green, M., Huang, S., Snaith, H.J., and Ho-Baillie, A. (2019). Fabrication of efficient and stable $CsPbI_3$ perovskite solar cells through cation exchange process. Adv. Energy Mater. *9*, 1901685. https://doi.org/10.1002/aenm.201901685.

42. Zhang, T., Wang, Y., Wang, X., Wu, M., Liu, W., and Zhao, Y. (2019). Organic salt mediated growth of phase pure and stable all-inorganic $CsPbX_3$ (X=I, Br) perovskites for efficient photovoltaics. Sci. Bull. *64*, 1773–1779. https://doi.org/10.1016/j.scib.2019.09.022.

43. Chen, Y., Lei, Y., Li, Y., Yu, Y., Cai, J., Chiu, M.H., Rao, R., Gu, Y., Wang, C., Choi, W., et al. (2020). Strain engineering and epitaxial stabilization of halide perovskites. Nature *577*, 209–215. https://doi.org/10.1038/s41586-019-1868-x.

44. Lee, J.W., Tan, S., Han, T.H., Wang, R., Zhang, L., Park, C., Yoon, M., Choi, C., Xu, M., Liao, M.E., et al. (2020). Solid-phase hetero epitaxial growth of alpha-phase formamidinium perovskite. Nat. Commun. *11*, 5514. https://doi.org/10.1038/s41467-020-19237-3.

45. Liu, M., Chen, Y., Tan, C.-S., Quintero-Bermudez, R., Proppe, A.H., Munir, R., Tan, H., Voznyy, O., Scheffel, B., Walters, G., et al. (2019). Lattice anchoring stabilizes solution-processed semiconductors. Nature *570*, 96–101. https://doi.org/10.1038/s41586-019-1239-7.

46. Steele, J.A., Jin, H., Dovgaliuk, I., Berger, R.F., Braeckevelt, T., Yuan, H., Martin, C., Solano, E., Lejaeghere, K., Rogge, S.M.J., et al. (2019). Thermal unequilibrium of strained black $CsPbI_3$ thin films. Science (New York, N.Y.) *365*, 679–684. https://doi.org/10.1126/science.aax3878.

47. Jiang, Q., Chu, Z., Wang, P., Yang, X., Liu, H., Wang, Y., Yin, Z., Wu, J., Zhang, X., and You, J. (2017). Planar-structure perovskite solar cells with efficiency beyond 21. Adv. Mater. *29*, 1703852. https://doi.org/10.1002/adma.201703852.

48. Zhao, Y., Ma, F., Qu, Z., Yu, S., Shen, T., Deng, H.-X., Chu, X., Peng, X., Yuan, Y., Zhang, X., and You, J. (2022). Inactive $(PbI_2)_2RbCl$ stabilizes perovskite films for efficient solar cells. Science (New York, N.Y.) *377*, 531–534. https://doi.org/10.1126/science.abp8873.

49. Shi, P., Ding, Y., Ding, B., Xing, Q., Kodalle, T., Sutter-Fella, C.M., Yavuz, I., Yao, C., Fan, W., Xu, J., et al. (2023). Oriented nucleation in formamidinium perovskite for photovoltaics. Nature *620*, 323–327. https://doi.org/10.1038/s41586-023-06208-z.

50. Liang, J., Han, X., Yang, J.H., Zhang, B., Fang, Q., Zhang, J., Ai, Q., Ogle, M.M., Terlier, T., Martí, A.A., and Lou, J. (2019). Defect-engineering-enabled high-efficiency all-inorganic perovskite solar cells. Adv. Mater. *31*, e1903448. https://doi.org/10.1002/adma.201903448.

51. Binek, A., Hanusch, F.C., Docampo, P., and Bein, T. (2015). Stabilization of the Trigonal High-Temperature Phase of Formamidinium Lead Iodide. J. Phys. Chem. Lett. *6*, 1249–1253. https://doi.org/10.1021/acs.jpclett.5b00380.

52. Qiu, Z., Li, N., Huang, Z., Chen, Q., and Zhou, H. (2020). Recent advances in improving phase stability of perovskite solar cells. Small Methods *4*, 1900877. https://doi.org/10.1002/smtd.201900877.

53. Lee, J.-W., Kim, D.-H., Kim, H.-S., Seo, S.-W., Cho, S.M., and Park, N.-G. (2015). Formamidinium and cesium hybridization for photo- and misture-stable perovskite solar cell. Adv. Energy Mater. *5*, 1501310. https://doi.org/10.1002/aenm.201501310.

54. Yi, C., Luo, J., Meloni, S., Boziki, A., Ashari-Astani, N., Grätzel, C., Zakeeruddin, S.M., Röthlisberger, U., and Grätzel, M. (2016). Entropic stabilization of mixed A-cation ABX_3 metal halide perovskites for high performance perovskite solar cells. Energy Environ. Sci. *9*, 656–662. https://doi.org/10.1039/c5ee03255e.

55. Park, Y.H., Jeong, I., Bae, S., Son, H.J., Lee, P., Lee, J., Lee, C.-H., and Ko, M.J. (2017). Inorganic Rubidium Cation as an Enhancer for Photovoltaic Performance and Moisture Stability of $HC(NH_2)_2PbI_3$ Perovskite Solar Cells. Adv. Funct. Mater. *27*, 1605988. https://doi.org/10.1002/adfm.201605988.

56. Xu, C., Chen, X., Ma, S., Shi, M., Zhang, S., Xiong, Z., Fan, W., Si, H., Wu, H., Zhang, Z., et al. (2022). Interpretation of rubidium-based perovskite recipes toward electronic passivation and ion-diffusion mitigation. Adv. Mater. *34*, e2109998. https://doi.org/10.1002/adma.202109998.

57. Kubicki, D.J., Prochowicz, D., Hofstetter, A., Zakeeruddin, S.M., Grätzel, M., and Emsley, L. (2017). Phase segregation in Cs-Rb- and K-doped mixed-cation $(MA)_x(FA)_{1-x}PbI_3$ hybrid perovskites from solid-state NMR. J. Am. Chem. Soc. *139*, 14173–14180. https://doi.org/10.1021/jacs.7b07223.

58. Saliba, M., Matsui, T., Seo, J.-Y., Domanski, K., Correa-Baena, J.-P., Nazeeruddin, M.K., Zakeeruddin, S.M., Tress, W., Abate, A., Hagfeldt, A., and Grätzel, M. (2016). Cesium-containing triple cation perovskite solar cells: improved stability, reproducibility and high efficiency. Energy Environ. Sci. *9*, 1989–1997. https://doi.org/10.1039/c5ee03874j.

59. Saliba, M., Matsui, T., Domanski, K., Seo, J.Y., Ummadisingu, A., Zakeeruddin, S.M., Correa-Baena, J.P., Tress, W.R., Abate, A., Hagfeldt, A., and Grätzel, M. (2016). Incorporation of rubidium cations into perovskite solar cells improves photovoltaic performance. Science (New York, N.Y.) *354*, 206–209. https://doi.org/10.1126/science.aah5557.

60. Masi, S., Gualdrón-Reyes, A.F., and Mora-Seró, I. (2020). Stabilization of Black Perovskite Phase in $FAPbI_3$ and $CsPbI_3$. ACS Energy Lett. *5*, 1974–1985. https://doi.org/10.1021/acsenergylett.0c00801.

61. Hu, M., Chen, M., Guo, P., Zhou, H., Deng, J., Yao, Y., Jiang, Y., Gong, J., Dai, Z., Zhou, Y., et al. (2020). Sub-1.4eV bandgap inorganic perovskite solar cells with long-term stability. Nat. Commun. *11*, 151. https://doi.org/10.1038/s41467-019-13908-6.

62. Jiang, Y., Yuan, J., Ni, Y., Yang, J., Wang, Y., Jiu, T., Yuan, M., and Chen, J. (2018). Reduced-dimensional α-$CsPbX_3$ perovskites for efficient and stable photovoltaics. Joule *2*, 1356–1368. https://doi.org/10.1016/j.joule.2018.05.004.

63. Li, B., Zhang, Y., Fu, L., Yu, T., Zhou, S., Zhang, L., and Yin, L. (2018). Surface passivation engineering strategy to fully-inorganic cubic CsPbI3 perovskites for high-performance solar cells. Nat. Commun. *9*, 1076. https://doi.org/10.1038/s41467-018-03169-0.

64. Zhao, X., Liu, T., Burlingame, Q.C., Liu, T., Holley, R., Cheng, G., Yao, N., Gao, F., and Loo, Y.-L. (2022). Accelerated aging of all-inorganic, interface-stabilized perovskite solar cells. Science (New York, N.Y.) *377*, 307–310. https://doi.org/10.1126/science.abn5679.

65. Jena, A.K., Kulkarni, A., Sanehira, Y., Ikegami, M., and Miyasaka, T. (2018). Stabilization of α-$CsPbI_3$ in ambient room temperature conditions by incorporating Eu into $CsPbI_3$. Chem. Mater. *30*, 6668–6674. https://doi.org/10.1021/acs.chemmater.8b01808.

66. Xiang, W., Wang, Z., Kubicki, D.J., Tress, W., Luo, J., Prochowicz, D., Akin, S., Emsley, L., Zhou, J., Dietler, G., et al. (2019). Europium-doped $CsPbI_2Br$ for stable and highly efficient inorganic perovskite solar cells. Joule *3*, 205–214. https://doi.org/10.1016/j.joule.2018.10.008.

67. Kubicki, D.J., Prochowicz, D., Pinon, A., Stevanato, G., Hofstetter, A., Zakeeruddin, S.M., Grätzel, M., and Emsley, L. (2019). Doping and phase segregation in Mn^{2+}- and Co^{2+}-doped lead halide perovskites from ^{133}Cs and ^{1}H NMR relaxation enhancement. J. Mater. Chem. A *7*, 2326–2333. https://doi.org/10.1039/c8ta11457a.

68. Akkerman, Q.A., Meggiolaro, D., Dang, Z., De Angelis, F., and Manna, L. (2017). Fluorescent alloy $CsPb_xMn_{1-x}I_3$ perovskite nanocrystals with high structural and optical stability. ACS Energy Lett. *2*, 2183–2186. https://doi.org/10.1021/acsenergylett.7b00707.

69. Bai, D., Zhang, J., Jin, Z., Bian, H., Wang, K., Wang, H., Liang, L., Wang, Q., and Liu, S.F. (2018). Interstitial Mn^{2+}-driven high-aspect-ratio grain growth for low-trap-density microcrystalline films for record efficiency $CsPbI_2Br$ solar cells. ACS Energy Lett. *3*, 970–978. https://doi.org/10.1021/acsenergylett.8b00270.

70. Hu, Y., Bai, F., Liu, X., Ji, Q., Miao, X., Qiu, T., and Zhang, S. (2017). Bismuth incorporation stabilized α-$CsPbI_3$ for fully inorganic perovskite solar cells. ACS Energy Lett. *2*, 2219–2227. https://doi.org/10.1021/acsenergylett.7b00508.

71. Xiang, S., Li, W., Wei, Y., Liu, J., Liu, H., Zhu, L., and Chen, H. (2018). The synergistic effect of non-stoichiometry and Sb-doping on air-stable alpha-$CsPbI_3$ for efficient carbon-based perovskite solar cells. Nanoscale *10*, 9996–10004. https://doi.org/10.1039/c7nr09657g.

72. Akman, E., Ozturk, T., Xiang, W., Sadegh, F., Prochowicz, D., Tavakoli, M.M., Yadav, P., Yilmaz, M., and Akin, S. (2023). The effect of B-site doping in all-inorganic CsPbIxBr3—x absorbers on the performance and stability of perovskite photovoltaics. Energy Environ. Sci. *16*, 372–403. https://doi.org/10.1039/D2EE01070D.

73. Lee, J.W., Dai, Z., Han, T.H., Choi, C., Chang, S.Y., Lee, S.J., De Marco, N., Zhao, H., Sun, P., Huang, Y., and Yang, Y. (2018). 2D perovskite stabilized phase-pure formamidinium perovskite solar cells. Nat. Commun. *9*, 3021. https://doi.org/10.1038/s41467-018-05454-4.

74. Li, N., Zhu, Z., Chueh, C.-C., Liu, H., Peng, B., Petrone, A., Li, X., Wang, L., and Jen, A.K.Y. (2017). Mixed cation $FA_xPEA_{1-x}PbI_3$ with enhanced phase and ambient stability toward high-performance perovskite solar cells. Adv. Energy Mater. *7*, 1601307. https://doi.org/10.1002/aenm.201601307.

75. Yoo, J.J., Seo, G., Chua, M.R., Park, T.G., Lu, Y., Rotermund, F., Kim, Y.-K., Moon, C.S., Jeon, N.J., Correa-Baena, J.-P., et al. (2021). Efficient perovskite solar cells via improved carrier management. Nature *590*, 587–593. https://doi.org/10.1038/s41586-021-03285-w.

76. Yoo, J.J., Wieghold, S., Sponseller, M.C., Chua, M.R., Bertram, S.N., Hartono, N.T.P., Tresback, J.S., Hansen, E.C., Correa-Baena, J.-P., Bulović, V., et al. (2019). An interface stabilized perovskite solar cell with high stabilized efficiency and low voltage loss. Energy Environ. Sci. *12*, 2192–2199. https://doi.org/10.1039/C9EE00751B.

77. Fan, Y., Chen, H., Liu, X., Ren, M., Liang, Y., Wang, Y., Miao, Y., Chen, Y., and Zhao, Y. (2023). Myth behind Metastable and Stable n-Hexylammonium Bromide-Based Low-Dimensional Perovskites. J. Am. Chem. Soc. *145*, 8209–8217. https://doi.org/10.1021/jacs.3c01684.

78. Li, H., Zhang, C., Gong, C., Zhang, D., Zhang, H., Zhuang, Q., Yu, X., Gong, S., Chen, X., Yang, J., et al. (2023). 2D/3D heterojunction engineering at the buried interface towards high-performance inverted methylammonium-free perovskite solar cells. Nat. Energy *8*, 946–955. https://doi.org/10.1038/s41560-023-01295-8.

79. Luo, L., Zeng, H., Wang, Z., Li, M., You, S., Chen, B., Maxwell, A., An, Q., Cui, L., Luo, D., et al. (2023). Stabilization of 3D/2D perovskite heterostructures via inhibition of ion diffusion by cross-linked polymers for solar cells with improved performance. Nat. Energy *8*, 294–303. https://doi.org/10.1038/s41560-023-01205-y.

80. Park, S.M., Wei, M., Xu, J., Atapattu, H.R., Eickemeyer, F.T., Darabi, K., Grater, L., Yang, Y., Liu, C., Teale, S., et al. (2023). Engineering ligand reactivity enables high-temperature operation of stable perovskite solar cells. Science (New York, N.Y.) *381*, 209–215. https://doi.org/10.1126/science.adi410.

81. Liao, J.-F., Rao, H.-S., Chen, B.-X., Kuang, D.-B., and Su, C.-Y. (2017). Dimension engineering on cesium lead iodide for efficient and stable perovskite solar cells. J. Mater. Chem. A *5*, 2066–2072. https://doi.org/10.1039/c6ta09582h.

82. Swarnkar, A., Marshall, A.R., Sanehira, E.M., Chernomordik, B.D., Moore, D.T., Christians, J.A., Chakrabarti, T., and Luther, J.M. (2016). Quantum dot-induced phase stabilization of alpha-$CsPbI_3$ perovskite for high-efficiency photovoltaics. Science *354*, 92–95. https://doi.org/10.1126/science.aag2700.

83. Yang, R.X., and Tan, L.Z. (2020). Understanding size dependence of phase stability and band gap in $CsPbI_3$ perovskite nanocrystals. J. Chem. Phys. *152*, 34702. https://doi.org/10.1063/1.5128016.

84. Alanazi, A.Q., Almalki, M.H., Mishra, A., Kubicki, D.J., Wang, Z., Merten, L., Eickemeyer, F.T., Zhang, H., Ren, D., Alyamani, A.Y., et al. (2021). Benzylammonium-mediated formamidinium lead iodide perovskite phase stabilization for photovoltaics. Adv. Funct. Mater. *31*, 2101163. https://doi.org/10.1002/adfm.202101163.

85. Akin, S., Akman, E., and Sonmezoglu, S. (2020). $FAPbI_3$-Based Perovskite Solar Cells Employing Hexyl-Based Ionic Liquid with an Efficiency Over 20% and Excellent Long-Term Stability. Adv. Funct. Mater. *30*, 2002964. https://doi.org/10.1002/adfm.202002964.

86. Min, H., Kim, M., Lee, S.-U., Kim, H., Kim, G., Choi, K., Lee, J.H., and Seok, S.I. (2019). Efficient, stable solar cells by using inherent bandgap of α-phase formamidinium lead iodide. Science *366*, 749–753. https://doi.org/10.1126/science.aay7044.

87. Huang, Z., Bai, Y., Huang, X., Li, J., Wu, Y., Chen, Y., Li, K., Niu, X., Li, N., Liu, G., et al. (2023). Anion–π interactions suppress phase impurities in $FAPbI_3$ solar cells. Nature *623*, 531–537. https://doi.org/10.1038/s41586-023-06637-w.

88. Bai, Y., Huang, Z., Zhang, X., Lu, J., Niu, X., He, Z., Zhu, C., Xiao, M., Song, Q., Wei, X., et al. (2022). Initializing film homogeneity to retard phase segregation for stable perovskite solar cells. Science (New York, N.Y.) *378*, 747–754. https://doi.org/10.1126/science.abn3148.

89. Liang, Z., Zhang, Y., Xu, H., Chen, W., Liu, B., Zhang, J., Zhang, H., Wang, Z., Kang, D.-H., Zeng, J., et al. (2023). Homogenizing out-of-plane cation composition in perovskite solar cells. Nature *624*, 557–563. https://doi.org/10.1038/s41586-023-06784-0.

90. Fu, Y., Rea, M.T., Chen, J., Morrow, D.J., Hautzinger, M.P., Zhao, Y., Pan, D., Manger, L.H., Wright, J.C., Goldsmith, R.H., and Jin, S. (2017). Selective stabilization and photophysical properties of metastable perovskite polymorphs of $CsPbI_3$ in thin films. Chem. Mater. *29*, 8385–8394. https://doi.org/10.1021/acs.chemmater.7b02948.

91. Jeong, B., Han, H., Choi, Y.J., Cho, S.H., Kim, E.H., Lee, S.W., Kim, J.S., Park, C., Kim, D., and Park, C. (2018). All-inorganic $CsPbI_3$ perovskite phase-stabilized by poly(ethylene oxide) for red-light-emitting diodes. Adv. Funct. Mater. *28*, 1706401. https://doi.org/10.1002/adfm.201706401.

92. Wang, Q., Zheng, X., Deng, Y., Zhao, J., Chen, Z., and Huang, J. (2017). Stabilizing the α-Phase of $CsPbI_3$ Perovskite by Sulfobetaine Zwitterions in One-Step Spin-Coating Films. Joule *1*, 371–382. https://doi.org/10.1016/j.joule.2017.07.017.

93. Fu, Y., Wu, T., Wang, J., Zhai, J., Shearer, M.J., Zhao, Y., Hamers, R.J., Kan, E., Deng, K., Zhu, X.Y., and Jin, S. (2017). Stabilization of the metastable lead iodide perovskite phase via surface functionalization. Nano Lett. *17*, 4405–4414. https://doi.org/10.1021/acs.nanolett.7b01500.

94. Liu, Y., Akin, S., Pan, L., Uchida, R., Arora, N., Milić, J.V., Hinderhofer, A., Schreiber, F., Uhl, A.R., Zakeeruddin, S.M., et al. (2019). Ultrahydrophobic 3D/2D fluoroarene bilayer-based water-resistant perovskite solar cells with efficiencies exceeding 22%. Sci. Adv. *5*, eaaw2543. https://doi.org/10.1126/sciadv.aaw2543.

95. Wang, Y., Zhang, T., Kan, M., Li, Y., Wang, T., and Zhao, Y. (2018). Efficient α-CsPbI3 photovoltaics with surface terminated organic cations. Joule *2*, 2065–2075. https://doi.org/10.1016/j.joule.2018.06.013.

96. Wang, Y., Zhang, T., Kan, M., and Zhao, Y. (2018). Bifunctional stabilization of all-inorganic alpha-$CsPbI_3$ perovskite for 17%

efficiency photovoltaics. J. Am. Chem. Soc. *140*, 12345–12348. https://doi.org/10.1021/jacs.8b07927.

97. Bian, H., Bai, D., Jin, Z., Wang, K., Liang, L., Wang, H., Zhang, J., Wang, Q., and Liu, S.F. (2018). Graded bandgap $CsPbI_{2+x}Br_{1-x}$ perovskite solar cells with a stabilized efficiency of 14.4. Joule *2*, 1500–1510. https://doi.org/10.1016/j.joule.2018.04.012.

98. Edri, E., Kirmayer, S., Kulbak, M., Hodes, G., and Cahen, D. (2014). Chloride Inclusion and Hole Transport Material Doping to Improve Methyl Ammonium Lead Bromide Perovskite-Based High Open-Circuit Voltage Solar Cells. J. Phys. Chem. Lett. *5*, 429–433. https://doi.org/10.1021/Jz402706q.

99. Xiao, J.W., Liang, Y., Zhang, S., Zhao, Y., Li, Y., and Chen, Q. (2019). Stabilizing $RbPbBr_3$ perovskite nanocrystals through Cs^+ substitution. Chem. Eur J. *25*, 2597–2603. https://doi.org/10.1002/chem.201805032.

100. Wang, Z., Zeng, L., Zhu, T., Chen, H., Chen, B., Kubicki, D.J., Balvanz, A., Li, C., Maxwell, A., Ugur, E., et al. (2023). Suppressed phase segregation for triple-junction perovskite solar cells. Nature *618*, 74–79. https://doi.org/10.1038/s41586-023-06006-7.

101. Braeckevelt, T., Goeminne, R., Vandenhaute, S., Borgmans, S., Verstraelen, T., Steele, J.A., Roeffaers, M.B.J., Hofkens, J., Rogge, S.M.J., and Van Speybroeck, V. (2022). Accurately determining the phase transition temperature of $CsPbI_3$ via random-phase approximation calculations and phase-transferable machine learning potentials. Chem. Mater. *34*, 8561–8576. https://doi.org/10.1021/acs.chemmater.2c01508.

102. McGehee, M.D. (2023). A sharp interface. Nat. Energy *8*, 224–225. https://doi.org/10.1038/s41560-023-01214-x.

103. Li, N., Niu, X., Li, L., Wang, H., Huang, Z., Zhang, Y., Chen, Y., Zhang, X., Zhu, C., Zai, H., et al. (2021). Liquid medium annealing for fabricating durable perovskite solar cells with improved reproducibility. Science (New York, N.Y.) *373*, 561–567. https://www.science.org/doi/abs/10.1126/science.abh3884.

104. Zhou, J., Xu, X., Wu, H., Wang, J., Lou, L., Yin, K., Gong, Y., Shi, J., Luo, Y., Li, D., et al. (2023). Control of the phase evolution of kesterite by tuning of the selenium partial pressure for solar cells with 13.8% certified efficiency. Nat. Energy *8*, 526–535. https://doi.org/10.1038/s41560-023-01251-6.

105. Henry, C.H. (2008). Limiting efficiencies of ideal single and multiple energy gap terrestrial solar cells. J. Appl. Phys. *51*, 4494–4500. https://doi.org/10.1063/1.328272.

106. Wang, Z., Zeng, L., Zhu, T., Chen, H., Chen, B., Kubicki, D.J., Balvanz, A., Li, C., Maxwell, A., Ugur, E., et al. (2023). Suppressed phase segregation for triple-junction perovskite solar cells. Nature *618*, 74–79. https://doi.org/10.1038/s41586-023-06006-7.

107. Werner, J., Sahli, F., Fu, F., Diaz Leon, J.J., Walter, A., Kamino, B.A., Niesen, B., Nicolay, S., Jeangros, Q., and Ballif, C. (2018). Perovskite/Perovskite/Silicon Monolithic Triple-Junction Solar Cells with a Fully Textured Design. ACS Energy Lett. *3*, 2052–2058. https://doi.org/10.1021/acsenergylett.8b01165.

108. Wang, S., Wang, P., Chen, B., Li, R., Ren, N., Li, Y., Shi, B., Huang, Q., Zhao, Y., Grätzel, M., and Zhang, X. (2022). Suppressed recombination for monolithic inorganic perovskite/silicon tandem solar cells with an approximate efficiency of 23. eScience *2*, 339–346. https://doi.org/10.1016/j.esci.2022.04.001.

109. Jošt, M., Köhnen, E., Al-Ashouri, A., Bertram, T., Tomšič, Š., Magomedov, A., Kasparavicius, E., Kodalle, T., Lipovšek, B., Getautis, V., et al. (2022). Perovskite/CIGS Tandem Solar Cells: From Certified 24.2% toward 30% and Beyond. ACS Energy Lett. *7*, 1298–1307. https://doi.org/10.1021/acsenergylett.2c00274.

110. Zheng, J., Wang, G., Duan, W., Mahmud, M.A., Yi, H., Xu, C., Lambertz, A., Bremner, S., Ding, K., Huang, S., and Ho-Baillie, A.W.Y. (2022). Monolithic Perovskite–Perovskite–Silicon Triple-Junction Tandem Solar Cell with an Efficiency of over 20. ACS Energy Lett. *7*, 3003–3005. https://doi.org/10.1021/acsenergylett.2c01556.

111. Eperon, G.E., Hörantner, M.T., and Snaith, H.J. (2017). Metal halide perovskite tandem and multiple-junction photovoltaics. Nat. Rev. Chem *1*, 95. https://doi.org/10.1038/s41570-017-0095.

112. Hörantner, M.T., Leijtens, T., Ziffer, M.E., Eperon, G.E., Christoforo, M.G., McGehee, M.D., and Snaith, H.J. (2017). The Potential of Multijunction Perovskite Solar Cells. ACS Energy Lett. *2*, 2506–2513. https://doi.org/10.1021/acsenergylett.7b00647.

113. Turedi, B., Yeddu, V., Zheng, X., Kim, D.Y., Bakr, O.M., and Saidaminov, M.I. (2021). Perovskite Single-Crystal Solar Cells: Going Forward. ACS Energy Lett. *6*, 631–642. https://doi.org/10.1021/acsenergylett.0c02573.

114. Zhumekenov, A.A., Saidaminov, M.I., Mohammed, O.F., and Bakr, O.M. (2021). Stimuli-responsive switchable halide perovskites: Taking advantage of instability. Joule *5*, 2027–2046. https://doi.org/10.1016/j.joule.2021.07.008.

115. Lin, J., Lai, M., Dou, L., Kley, C.S., Chen, H., Peng, F., Sun, J., Lu, D., Hawks, S.A., Xie, C., et al. (2018). Thermochromic halide perovskite solar cells. Nat. Mater. *17*, 261–267. https://doi.org/10.1038/s41563-017-0006-0.

116. Li, Z., Klein, T.R., Kim, D.H., Yang, M., Berry, J.J., van Hest, M.F.A.M., and Zhu, K. (2018). Scalable fabrication of perovskite solar cells. Nat. Rev. Mater. *3*, 18017. https://doi.org/10.1038/natrevmats.2018.17.

117. Li, H., Zhou, J., Tan, L., Li, M., Jiang, C., Wang, S., Zhao, X., Liu, Y., Zhang, Y., Ye, Y., et al. (2022). Sequential vacuum-evaporated perovskite solar cells with more than 24% efficiency. Sci. Adv. *8*, eabo7422. https://doi.org/10.1126/sciadv.abo7422.

118. Liu, X., Luo, D., Lu, Z.-H., Yun, J.S., Saliba, M., Seok, S.I., and Zhang, W. (2023). Stabilization of photoactive phases for perovskite photovoltaics. Nat. Rev. Chem *7*, 462–479. https://doi.org/10.1038/s41570-023-00492-z.

119. Jiang, Y., Remeika, M., Hu, Z., Juarez-Perez, E.J., Qiu, L., Liu, Z., Kim, T., Ono, L.K., Son, D.-Y., Hawash, Z., et al. (2019). Negligible-Pb-Waste and Upscalable Perovskite Deposition Technology for High-Operational-Stability Perovskite Solar Modules. Adv. Energy Mater. *9*, 1803047. https://doi.org/10.1002/aenm.201803047.